Journal of Multidisciplinary Engineering Science and Technology (JMEST)
ISSN: 2458-9403
Vol. 6 Issue 3, March - 2019

Effect Of Corrugated Metal Sheet Roof Vicinity On Performance Of Outdoor Mounted Polycrystalline Silicon Solar PV Module

Nickson John[1,2]
[2]Department of Electrical Engineering, Arusha Technical College
Arusha, Tanzania
johnn@nm-aist.ac.tz

Tatiana Pogrebnaya[1]
[1]Department of Materials and Energy Science and Engineering, Nelson Mandela African Institution of Science and Technology
Arusha, Tanzania.
tatiana.pogrebnaya@nm-aist.ac.tz

Thomas Kivevele[1]
[1]Department of Materials and Energy Science and Engineering, Nelson Mandela African Institution of Science and Technology
Arusha, Tanzania
thomas.kivevele@nm-aist.ac.tz

***Abstract*—Experimental and theoretical performance analysis of standalone solar photovoltaic (PV) module was done at tropical area; the influence of corrugated metal sheet (CMS) roof vicinity on the PV module performance was the focus of the study. The module of 100 watts was placed on a simple developed CMS roof structure with variable gap between the roof and PV panel. Electrical circuit with data acquisition system was designed based on Proteus and Arduino technologies. Solar irradiance, ambient air temperature and humidity, temperature of the panel, current and voltage were monitored.**

In the view of findings, the PVs' extra heat was originating from corrugated metal sheet roof vicinity. The highest temperature attained by the PV panel when it was directly mounted on the roof was 74.5 °C while the ambient temperature was 32 °C and irradiance of 820 ± 10 Wm-2. The PVs' temperature dropped by ~9 °C and output power increased by ~11% when the gap enlarged from 0 to 50 cm at the same irradiance. The monitored experimental parameters were used as the inputs for the Matlab simulation. Experimental and simulated I-V curves were in good correlation hence validating the findings.

Keywords*—PV - corrugated metal sheet gap, gap temperature, module temperature, short circuit current, open circuit voltage, maximum power.

Nomenclature

CMS - corrugated metal sheet
G – irradiance (Wm^{-2})
h – length gap between PV and corrugated metal sheet (cm)
I_{SC} – short circuit current (A)
T_a – ambient temperature (°C)
T_g – temperature in the gap between PV and corrugated metal sheet roof (°C)
T_m – module rear surface temperature (°C)
T_S – temperature of corrugated metal sheet front surface (°C)
V_{OC} - open circuit voltage (V)

1. INTRODUCTION

Rural electrification and rural development have largely been restricted to grid extension by utilities with limited coverage of decentralized electricity possibilities. Increased population and significant change in pattern of trade and financial sector; rural electrification by solar energy can be among crucial factors for a rural community's development. Solar energy is one of the paramount renewable energy resources with minutest deleterious effects on the environment. It is a resource that spreads the earth as sunlight that exists worldwide compared to other renewable energy resources which are site specific. Sunlight reaching our environment can be rehabilitated into electricity directly by PV cell technology. Hence, using electricity produced by solar PV system in domestic applications, particularly in places which receive plentiful solar irradiance like Tanzania, is amongst of the paramount solution for rural electrification [1][2][3][4][5][6][7][8][9][10].

The performance of solar PV panel is influenced by excessive cell temperature and is directly proportional to the irradiance reaching the cell. Outdoor roof mounted solar PV module's temperature varies depending on ambient temperature, level of sunlight, and roofing material [11][12]. The increase in module's temperature lowers the efficiency of PVs [13][14]. The impacts of increased temperature on solar cell are exposed by the I-V and P-V curves [13][15][16][17]. The output of the solar PV module would be increased by optimizing the orientation and allowing free natural air movement on the rear surface of the PV [18][19]. Most of remote rural roof installed solar PV modules are done on the pitched roof structure whilst gaps for free air flow and proper orientation are not carefully experimented (Fig. 1).

Fig. 1: Solar PVs mounted with different PV-roof spacing

Numerous studies have been done to assess the performance of solar PV module but none of them has quantified and mitigated the effect of PV and roof variance. Mattei, Notton, Cristofari, Muselli, and Poggi [20] exposed that variations of surrounding temperature, solar irradiance, and wind speed affected the module's electrical output parameters. Khan, Nyari, Park , and Kim [21] reported that the net electric power delivered by the solar PV module decreased due to high operating temperature under the same solar irradiance condition and with decreasing solar radiation. Fesharaki, Dehghani, and Tavasoli [13] revealed that the efficiency decreased with temperature increase and fluctuate with irradiance. Therefore, the efficiency of solar PV depends on environmental, geographical and technical factors. Poor mounting, improper orientation, fewer irradiance capture by PV cell, and great PV's operating temperature are the factors reported to affect module power output [22][23][24][16][25].
Despite the fact that a significant number of studies have reported performance of PV modules but none of them has quantified outdoor experimental performance of standalone solar PV modules in terms of the influence of PV -pitched roof gap in the area of study. Therefore, the aim of this study was to investigate and analyze outdoor performance of polycrystalline silicon solar module mounted on pitched corrugated metal sheet (CMS) roof which is mostly used as a roofing material. To examine the impact of the CMS, the PV module performance was monitored at different gap size, from 0 to 50 cm, between the top roof pitch and the PV.

2. MATERIALS AND METHODS

2.1 Equipment and Accessories

Equipment and accessories listed below were used in this study: solar PV module (100 W) for conversion of solar irradiance to electricity, mounting structure serving as house roof and support for solar PV module, corrugated metal sheet roof for examining the effect of temperature on PV performance, data acquisition system to measure current and voltage. Other meters were used to monitor the parameters: temperatures of the module, gap and CMS - USB SSN-11e, air temperature and humidity - USB SSN-22e, solar irradiance - USB TES 132 solar power meter, and wind speed - kestrel.

Mounting structure was made by square mild steel hollow sections; roofing was done by corrugated metal sheet "AL-ZN gauge 30 AZ-85" type. Data acquisition system was designed to read and record required parameters of the study using electronic components like switching transistor, resistors, diodes, relay, real time clock, voltage sensor, current sensor, linear monolithic sensors, secure digital card and card reader which were fixed and soldered on single sided copper clad board (Fig. 2). Mega Arduino development board was used for integrating the components readouts whilst liquid crystal display was also incorporated to enable visual readouts. The circuit was designed by the use of Proteus and Arduino technologies while C language was used to program the circuit. The circuit was fixed in housing and powered by a 9 V battery. The PV module energy collector surface was 0.75 m^2 with 36 numbers of cells; the characteristics of the module at standard test conditions (STC) provided from manufacturers are listed in Table 1 with tolerance of ~ ± 3%.

Table 1: Characteristics of solar panel

Characteristics	***Amount***
Maximum power (W)	100
DC open circuit voltage (V)	22.14
DC maximum power point voltage (V)	18.5
DC short circuit current (A)	5.78
DC maximum power point current (A)	5.43
Nominal operating cell temperature (°C)	47±2
Temperature coefficient of P_{max} (W/°C)	-0.45
Temperature coefficient of V_{OC} (V/°C)	-0.35
Temperature coefficient of I_{SC} (A/°C)	0.04

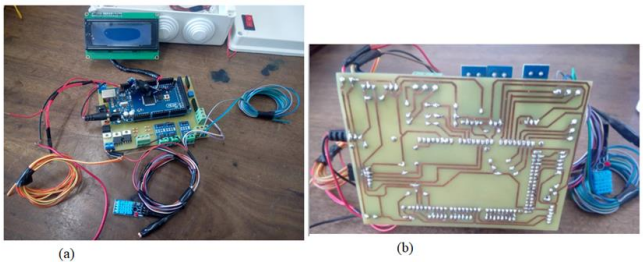

Fig. 2: Clad board circuit with soldered components connections; (a) Circuit front view; (b) Circuit back view

2.2 Experimental Setup

Experiments were done on a pitched corrugated metal sheet with variable gap between the roof and PV module (Fig. 3). It was set on ground at Nelson Mandela African Institution of Science and Technology located at 03.40° south and 36.79° east at the altitude of 1206 meters from sea level facing north to the equator. The poles of module holder was fixed at 15° panel's tilt angle adopted from review by Jacobson & Jadhav [26]; the selected module inclination was appropriate for the experiments where

was conducted. The poles were made to move up and down for changing the gap between the CMS and module.

The USB SSN-22e data logger sensors were hanged at the mounting structure. Two sets of temperature sensors were used, one linear monolithic sensor and one USB SSN-11e sensor, for measuring each of the temperatures: T_m - module rear surface temperature; T_g - in the gap between PV and CMS, and T_S - CMS front surface temperature. The experimental temperature values dissimilarities from the two sets of sensors were within ± 3% which is inconsequential difference and confirmed reliability of the data achieved. Solar power meter was set at same inclination as the solar PV module to receive and record the same amount of solar energy. Kestrel wind speed meter was fixed perpendicular to the mounting structure where current and voltage were recorded by data acquisition system.

Each solar PV module was cleaned to remove any dusts contaminated on energy collector surface before the start of the experiments. The experiments were conducted from 27th August 2018 to 18th of November 2018 commencing at hours with clear sky.

2.3 Experimental Measurements and Matlab simulation

To evaluate the impact of CMS on the solar PV module performance, the measurements of electrical and other parameters were done at different gaps *h* between the module and CMS. The size of the gap was varied manually; from 0 to 50 cm with the step of 10 cm. The solar irradiance ***G***, ambient air temperature T_a and relative humidity *Rh*, as well as temperatures of the module T_m, roof surface T_S, and within the gap T_g, were examined and continuously recorded after every two minutes.

Fig. 3: Experimental setup: PV module attached to CMS and temperature sensors

To get currents and voltages for I-V curves, the string of load resistances was connected to the module as depicted in Fig. 4a. The PV module was monitored at irradiance of 480±10, 680±10, and 820±10 Wm^{-2}. The readings of digital multimeters were captured by digital camera as depicted in Fig. 4b.

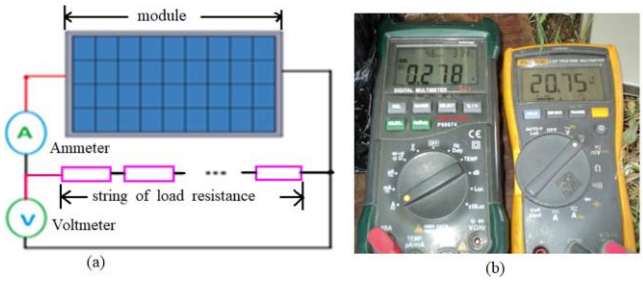

Fig. 4: Electrical characteristics measurement; (a) Circuit diagram for I-V curves measurements; (b) I-V experimental data collection

The experimental data were then used as an input variable data for Matlab simulation. A generalized model of a solar PV cell was implemented; the equivalent circuit consisting of a current source (PV cell) connected in parallel with a diode (D), and shunt resistance (R_P), as well as series resistance (Rs), is shown in Fig. 5. The photo current I_{PV} of solar PV cell was calculated based on equations (1) and (2) [27].

$$Ipv = Id + Ip + Io \quad (1)$$

$$Voc = \frac{nkT}{q}\ln\left[\left(\frac{Ipv}{Id}\right) + 1\right] \quad (2)$$

where I_d is diode (cell) saturation current, I_p is a shunt current and I_o is a output (load) current, *n is the* ideality constant of the diode (*n* = 1.3 for silicon polycrystalline), *k* is a Boltzmann's constant (*k* = 1.38 x 10^{-23} J/°K), *q* is an electron charge (*q* = 1.602 x 10^{-19} C).

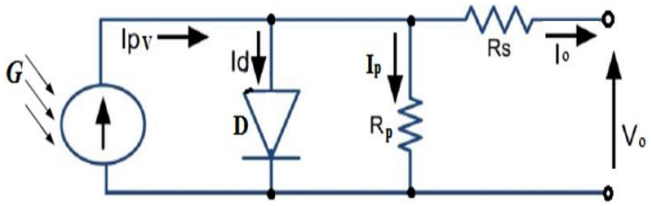

Fig. 5: Solar PV cell equivalent circuit

3. Results and Discussion

3.1 *Variation of the system temperature with solar irradiance*

The data recorded and considered for analysis were those taken at clear sky condition when less irradiance variations was expected as compared to cloudy hours. The module was fixed directly on CMS roof. Weather parameters; irradiance ***G***, ambient temperature T_a and relative humidity *Rh*, as well as temperature of CMS T_S, were recorded as depicted in Fig. 6 in ascend sorted. Either T_a, T_S, or *Rh* displayed small influence by solar radiation; temperature increases and humidity decreases with irradiance escalation but not substantially. The readouts ranged from ~29 °C – 36 °C for T_a, ~55°C - 70°C for T_S and about ~33% to 51% for Rh throughout test day. It was noted that any drop in T_S whilst irradiance was keeping increasing was due to an upswing in humidity and increased wind blowing, from 0 to 2.7 ms^{-1}. It is

worth to mention about challenging to carry experiments due to the variation of irradiance reaching the solar module; this observation concurs with Sirisamphanwong & Ketjoy [28] study.

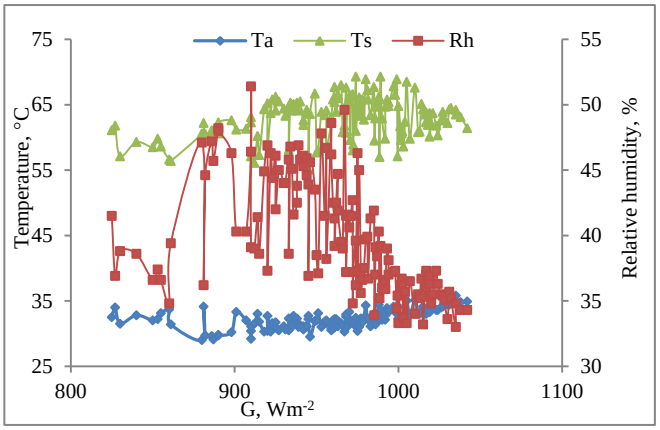

Fig. 6: Variation of ambient temperature Ta, roof sheet temperature T_S, and relative humidity Rh versus irradiance

It is apparently that CMS roof is heat absorbing material. The highest were T_S 62 °C, T_g 48 °C and T_m 74.5 °C whilst T_a was ranging from 21-35 °C (Fig. 7). For every sudden increase in T_m also there was high pitched increase in T_S but only insignificant escalation in T_g. Regarding the time of a day, lower temperatures T_S, T_g, and T_m observed before 10:30 hours and after 15:00 hours compared to noon time. It is obviously the rise of T_m was promoted by lack of air exchange on the rear side because the roof material radiated quickly and contributed to increase in the module temperature T_m as the space was not well ventilated. This result is in accordance with the findings reported by [16, 28]. Fluctuations for monitored parameters were due change in environmental conditions caused by either among the following; increased or decreased wind speed, un-prolonged cloud cover, or irradiance fluctuations which was ranging from 300 -1150 Wm^{-2}.

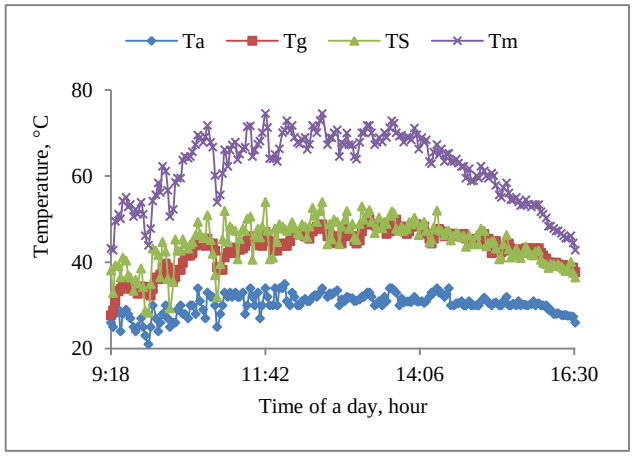

Fig. 7: Variations of temperatures versus time of a day

The effect of solar irradiance on the PV module temperature is seen in Fig. 8. The plot shows a definite arising trend with irregular oscillations. Temperature fluctuations can be attributed to surrounding temperature and wind speed variations. While ambient temperature T_a was in a range of 21-35 °C; the module temperature T_m exceeded it by 17 - 42 °C that is much higher than usually putative about 15 °C. This higher T_m can be attributed to negligible PV-roof gap that actually brings extra heating to the module. Similar findings were reported in Kaldellis, Kapsali, and Kavadias [16]; that modules works at diverse range of temperature whereas 70 °C is come across and this persisted due to poor cooling.

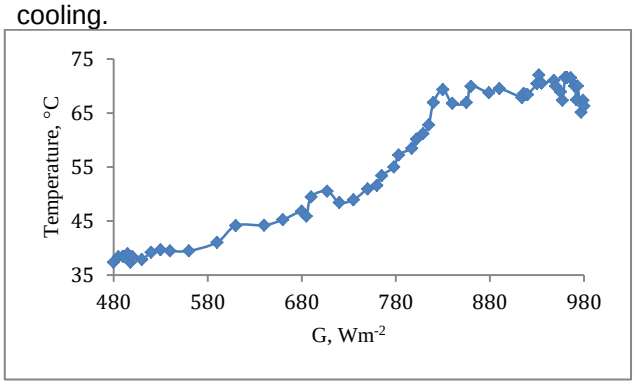

Fig. 8: Module's temperature variation versus irradiance

3.2 *Solar PV performance with panel mounted directly on the roof*

The effect of solar radiation on solar PV module electrical performance was examined, results are plotted Fig. 9. The short circuit currents I_{SC} grow linearly with irradiance increase whilst voltages drop by 0.7-1.0 V at irradiance approaching 820 Wm^{-2} (Fig.9a). These results are in accord to linear relation of current to illumination equation (3).

$$I(G) = \left(\frac{G}{Go}\right)[Io(Go)] \qquad (3)$$

where *Go* is 1 kWm^{-2} at AM 1.5, I_o *(Go)* cell current at *Go*; and logarithmic dependence of voltage [23].

Fig. 9b shows electrical characteristic curves measured and displayed at distinct irradiances. Monitored values of maximum power obtained from the curves were plotted against irradiance in Fig. 9c. It is clear that when solar radiation escalated, the I_{SC} and maximum power P_{max} were snowballing due to improved number of photons reaching the module.

One can notice the interrelation between the parameters that the output power is mostly influenced by current change and least by voltage whilst currents and voltages (and hence net power) were affected by solar irradiance and also by the module temperature T_m. The results accord with theoretical studies [15][30][31][32] that with escalating in working module temperature T_m, the I_{SC} increases whilst V_{OC} and P_{max} decline. Generally, experimental electrical characteristic tests outcomes were fluctuating due to variation of solar radiation that varied from morning to afternoon as also observed by Sirisamphanwong and

Ketjoy [28]. Descent in solar insolation resulted to for a reduction in I_{SC}, V_{OC}, T_m, and T_a readouts. Alike observations were reported by J. C. Arjyadhara and Ali [33] that with the increasing solar insolation I_{SC} increases, and V_{OC} decreases, and hence electrical characteristic curves varies.

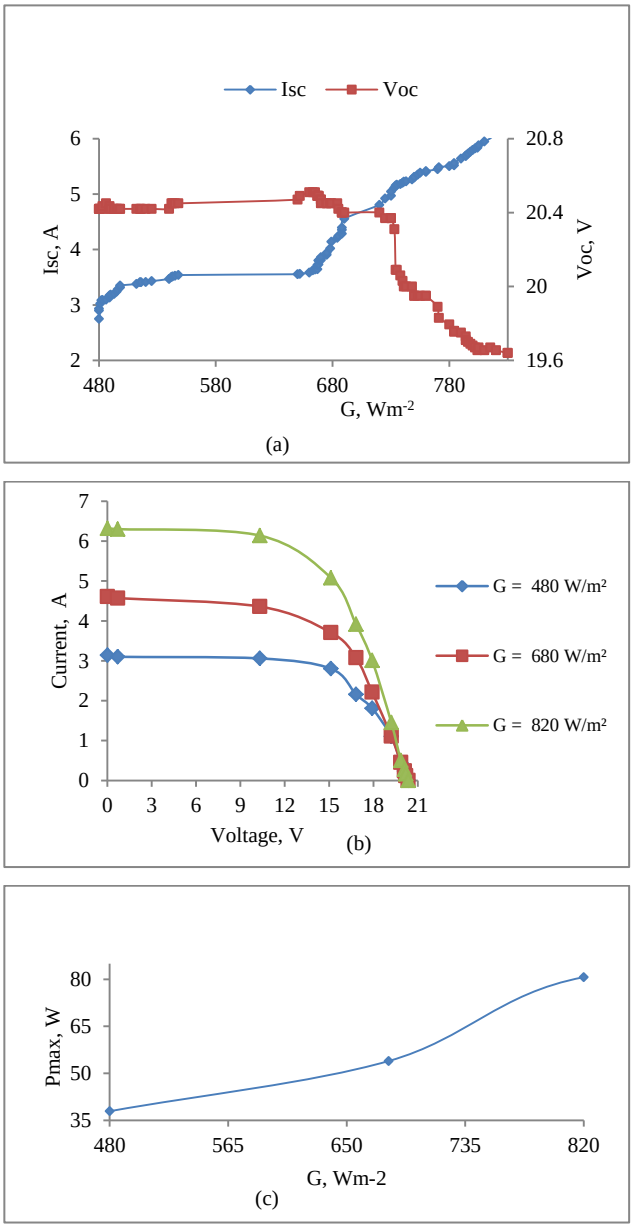

Fig. 9: Performance of solar module at different irradiance; (a) Short circuit current and open circuit voltage versus irradiance; (b) I-V curves; (c) Variation of maximum power versus irradiance

3.3 Impact of gap variance on PV performance

The effects of gap size between the CMS roof and module on temperatures T_a, T_g, T_m, and output maximum power P_{max} are depicted in Fig. 10. The monitored parameters were obtained at G = 820±10 Wm^{-2} of the same day; the gap size *h* was varied from 0 to 50 cm.

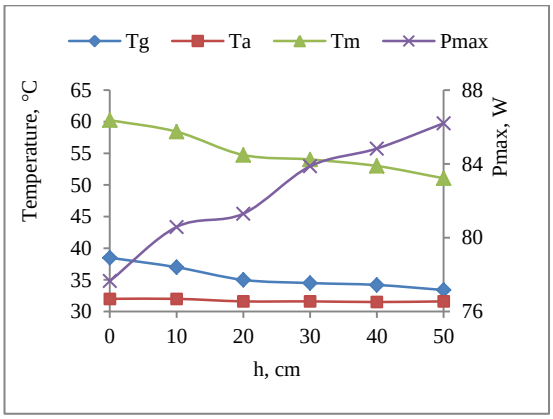

Fig. 10: Temperatures and power P_{max} variations depending on gap alteration from h = 0 to 50 cm at G = 820±10 Wm^{-2}

One can see that, the T_g and T_m decreased regularly while P_{max} raised steadily with the gap enlargement; at the same time the ambient temperature T_a was not varying. The relationship maintained $T_a < T_g < T_m$ along with the gap alteration; this result concurs with Dominguez, Kleissl, and Luvall [29], the gap temperature T_g approached the ambient one T_a at *h* = 50 cm. The T_g was decreasing as the gap rising. It was observed that, mounting the panel at 50 cm gap reduced the module temperature T_m up to 21% depending on solar radiation, and increased the net output power up to 11% compared to the module laid directly on the CMS roof.

The measured temperature T_m can be compared to values obtained theoretically through equation (4) [23][34].

$$Tc = Ta + (NOCT - 25) \times \left(\frac{G}{Go}\right) \qquad (4)$$

Where *Tc* is cell temperature and NOCT is the nominal operating cell temperature at ambient temperature of 25 °C, AM 1.5 and irradiance *Go* = 1000 Wm^{-2}. The computation of the cell temperature using equation (4), yielded the T_m in range of 48.4 °C to 51.7 °C depending on G and T_a. At 50 cm gap, the T_a was 32 °C and G was 820 Wm^{-2}, the measured T_m was in a computed range. For 0 cm gap, the T_m was in the range of 54 °C to 60 °C; moreover it could go beyond that if the module is left for long time. Disagreement between the computed and measured at zero gap temperatures might be attributed due extra heat from roofing material and the lack of air exchange on the module rear side. A similar findings on ventilation were reported by Skoplaki and Palyvos [35] that, higher T_m was due to improper cooling that resulted from poor ventilated module backside.

The performances of solar PV are depicted in Fig. 11; current at maximum power I_{mp} and open circuit voltage V_{OC} are shown versus gap size *h* in Fig. 11a and I-V and P-V curves in Fig. 10b. With the gap expand from 0 to 50 cm, maximum power current (I_{mp}) slightly ascended with the gap enlarges and V_{OC} was increasing. I-V as well as P-V curves depicted in Fig.

11b appear close to each other and over-crowding hence curves for 0, 20 cm and 50 cm gap are shown. The increase in voltage was significant to increase net power output. It is worth to note that our output electrical parameters measured at G = 820 Wm^{-2} and *h* = 50 cm; were I_{SC} = 6.2 A, V_{OC} = 20.7 V and P_{max} = 86.2 W; were close those obtained at standard condition as reported by the manufacturer (Table 1). According to Chikate and Sadawarte [25] the module was supposed to generated at least 86.33 W after considering the effect of tolerance and a recommended typical temperature reduction factor.

The efficiency η and fill factor *FF* were calculated from equations (5) and (6);

$$\eta = \frac{P_{max}}{G\,A} \quad (5)$$

$$FF = \frac{P_{max}}{V_{oc}\,I_{sc}} \quad (6)$$

where *A* is module area; and portrayed via bar diagram versus gap *h* in Fig. 12. With gap enlarge; the efficiency η rose from 12.7% to 14.1%; the *FF* rose slightly from 61% to 71% that is bit less to the manufacturer, 78%.

Concluding this section about the gap *h* impact on the module performance, it worth to mention the module temperature concern. The values of V_{OC}, *FF*, and P_{max} declined with temperature but I_{SC} rose. It is in accordance with the temperature coefficients which are negative for V_{OC}, and P_{max} while positive for the I_{SC} (Table 1).

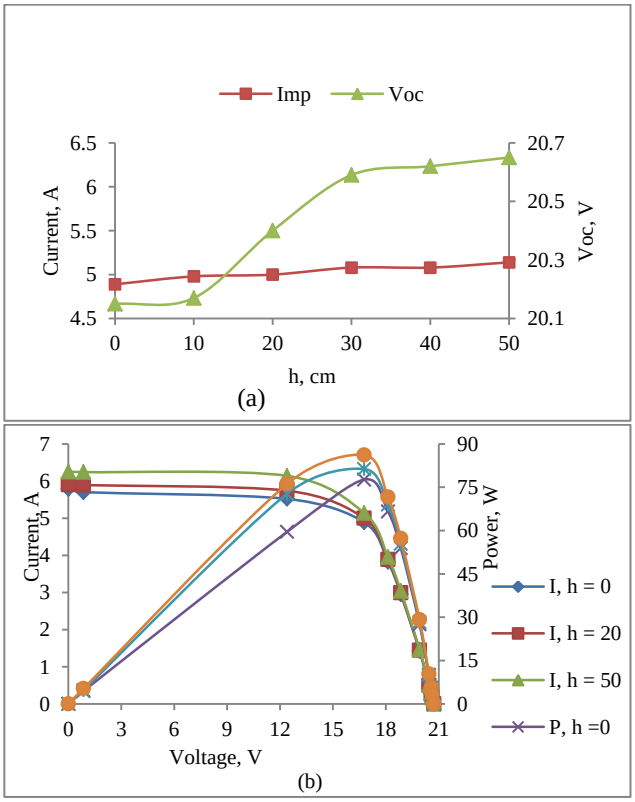

Fig. 3: Solar module performance at irradiance 820±10 Wm^{-2} for 0-50 cm gap alteration; (a) Short circuit current, current at maximum power and open circuit voltage; (b) I-V and P-V curves

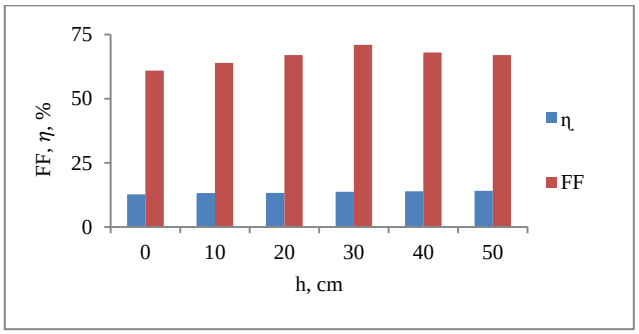

Fig. 42: Impact of a gap h between the solar panels and roof on the panels' performance measured outdoor at solar irradiance 820±10 Wm^{-2}

3.4. Comparison of experimental and simulated results

In order to test the validity of the results, the comparisons between the experimental and simulated data were carried out. Experimental T_m, electrical parameters and irradiance measured during experiment were used as input data to the Matlab function and command codes. Plotting electrical characteristic curves of the module cells for a certain working irradiance and certain module cell temperature, one of them was fixed while another one varied [36]. The simulated parameters were evaluated using the basic equations (1) and (2) of generalized model for equivalent circuit (Fig. 5).

The simulated I-V curves computed at different irradiances are given in Fig. 13. With increase of solar irradiance, the I_{SC} of the module increases, which is in accords with equation (3); the short circuit current is directly proportional to the radiant intensity. The open circuit voltage decreases as slightly as it is logarithmically relate to solar irradiance.

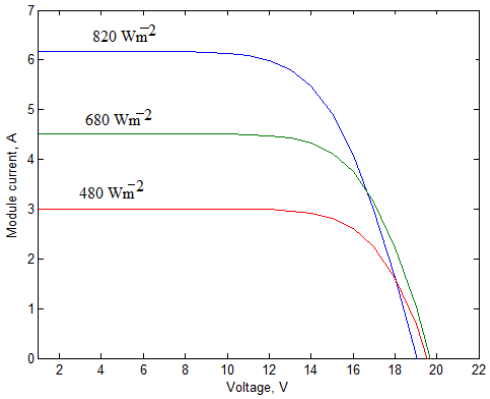

Fig. 5: Simulated I-V curves at different irradiance

The simulated results are compared to experimental I-V curves (Fig. 14) obtained at different irradiances and (*h* = 0). In general, a very good agreement is observed between the experimental and the simulated results hence validating the findings.

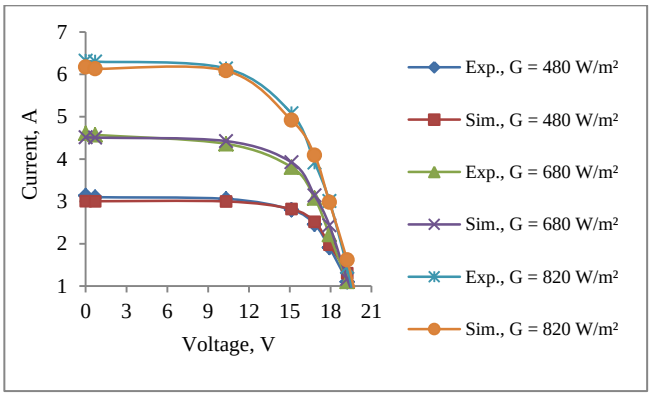

Fig. 6: Simulated and experimental current-voltage curves (h= 0)

4. CONCLUSION

The impact of corrugated metal sheet vicinity on the PV module temperature and electrical characteristics was examined outdoor under different solar irradiance and gap size between the module and roof. When the module was laid directly on the roof, the temperature of the module exceeded the ambient one by 17 - 42 °C depending on the irradiance that was much higher than usually accepted about 15 °C for standalone PV system. With the gap enlarge from 0 to 50 cm, the module temperature reduced by 9%, and the power output was raised by 11%. Apparently the PV extra heating originated from roof vicinity; in spite the roof temperature appeared lower by ~5-29 °C than that of the module. A gap between the roof surface and module was helpful to reduce extra heat on the module and increase the power; the large size of the gap favored better performance of the module. Therefore, PVs mounted at least 50 cm above the corrugated metal sheet could operate within nominal operating cell temperature and generate good power. Simultaneous monitoring of the module's performance revealed rather synchronous behavior of temperatures and electrical parameters regarding change in irradiance or gap size that confirms reliability of the results obtained. Experimental and simulated I-V curves were in good agreement. A similar study can be recommended to investigate the influence of different roofing materials on PV performance.

CONFLICTS OF INTEREST

The authors proclaim no conflicts of interest concerning the publication of this paper.

REFERENCE:

[1] A. Mellit, S. A. Kalogirou, S. Shaari, H. Salhi, and A. Hadj Arab, "Methodology for predicting sequences of mean monthly clearness index and daily solar radiation data in remote areas: Application for sizing a stand-alone PV system," *Renew. Energy*, vol. 33, no. 7, pp. 1570–1590, 2008.

[2] S. Szabo´, K. B'odis, T. Huld, and M. Moner-Girona, "Energy solutions in rural Africa : mapping electrification costs of distributed solar and diesel generation versus grid extension *," *Environ. Res. Lett.*, 2011.

[3] B. Parida, S. Iniyan, and R. Goic, "A review of solar photovoltaic technologies," *Renew. Sustain. Energy Rev.*, vol. 15, no. 3, pp. 1625–1636, 2011.

[4] K. H. Solangi, M. R. Islam, R. Saidur, N. A. Rahim, and H. Fayaz, "A review on global solar energy policy," *Renew. Sustain. Energy Rev.*, vol. 15, no. 4, pp. 2149–2163, 2011.

[5] S. Kihwele, K. Hur, and A. Kyaruzi, "Visions, Scenarios and Action Plans Towards Next Generation Tanzania Power System," *Energies*, pp. 3908–3927, 2012.

[6] J. Ondraczek, "The sun rises in the east (of Africa): A comparison of the development and status of solar energy markets in Kenya and Tanzania," *Energy Policy*, vol. 56, pp. 407–417, 2013.

[7] V. Khare, S. Nema, and P. Baredar, "Status of solar wind renewable energy in India $," *Renew. Sustain. Energy Rev.*, vol. 27, pp. 1–10, 2013.

[8] H. Ahlborg and L. Hammar, "Drivers and barriers to rural electrification in tanzania and mozambique - grid-extension, off-grid, and renewable energy technologies," *Renew. Energy*, vol. 61, pp. 117–124, 2014.

[9] E. A. Nyari, T. Pogrebnaya, and L. Wilson, "Energy Sector and Solar Energy Potential in Tanzania," *International Journal Emerging. Technol. Eng.*, vol. 2, no. 9, pp. 2348–8050, 2015.

[10] T. Kulworawanichpong and J. J. Mwambeleko, "Design and costing of a stand-alone solar photovoltaic system for a Tanzanian rural household," *Sustain. Energy Technology. Assessments*, vol. 12, pp. 53–59, 2015.

[11] C. Honsberg and S. Bowden, "Nominal Operating Cell Temperature," *Pvcdrom*, 2014. [Online]. Available: http://www.pveducation.org/pvcdrom/modules/nominal-operating-cell-temperature. [Accessed: 05-Mar-2018].

[12] C. Honsberg and S. Bowden, "Heat Loss in PV Modules | PVEducation," 2016. [Online]. Available:http://www.pveducation.org/pvcdrom/modules/heat-loss-in-pv-modules. [Accessed: 06-Mar-2018].

[13] V. J. Fesharaki, M. Dehghani, J. J. Fesharaki, and H. Tavasoli, "The Effect of Temperature on Photovoltaic Cell Efficiency," *Proceeding 1st Int. Conf. Emerg. Trends Energy Conserv.*, no. November, pp. 20–21, 2011.

[14] S. Dubey, J. N. Sarvaiya, and B. Seshadri, "Temperature dependent photovoltaic (PV) efficiency and its effect on PV production in the world - A review," *Energy Procedia*, vol. 33, pp. 311–321, 2013.

[15] V. V Tyagi, N. A. A. Rahim, N. A. Rahim, and J. A. L. Selvaraj, "Progress in solar PV technology : Research and achievement," *Renew. Sustain. Energy Rev.*, vol. 20, pp. 443–461, 2013.

[16] J. K. Kaldellis, M. Kapsali, and K. A. Kavadias, "Temperature and wind speed impact on the ef fi ciency of PV installations . Experience obtained from outdoor measurements in Greece," *Renew. Energy*, vol. 66, pp. 612–624, 2014.

[17] S. Chander, A. Purohit, A. Sharma, S. P. Nehra, and M. S. Dhaka, "A study on photovoltaic parameters of mono-crystalline silicon solar cell with cell temperature," *Energy Reports*, vol. 1, pp. 104–109, 2015.

[18] J. Gooding, R. Crook, and A. S. Tomlin, "Modelling of roof geometries from low-resolution LiDAR data for city-scale solar energy applications using a neighbouring buildings method," *Appl. Energy*, vol. 148, pp. 93–104, 2015.

[19] T. Stathopoulos, "Wind loads on low buildings: In the wake of Alan Davenport's contributions," *J. Wind Eng. Ind. Aerodyn.*, vol. 91, no. 12–15, pp. 1565–1585, 2003.

[20] M. Mattei, G. Notton, C. Cristofari, M. Muselli, and P. Poggi, "Calculation of the polycrystalline PV module temperature using a simple method of energy balance," *Renew. Energy*, vol. 31, pp. 553–567, 2006.

[21] M. Khan, B. Ko, E. A. Nyari, S. E. P. Park, and H.-J. Kim, "Performance Evaluation of Photovoltaic Solar System with Different Cooling Methods and a Bi-Reflector Comparative Analysis," *energies*, vol. 10, no. 826, p. 23, 2017.

[22] M. E. Meral and F. Diner, "A review of the factors affecting operation and efficiency of photovoltaic based electricity generation systems," *Renew. Sustain. Energy Rev.*, vol. 15, no. 5, pp. 2176–2184, 2011.

[23] S. Mekhilef, R. Saidur, and M. Kamalisarvestani, "Effect of dust, humidity and air velocity on efficiency of photovoltaic cells," *Renew. Sustain. Energy Rev.*, vol. 16, no. 5, pp. 2920–2925, 2012.

[24] V. Sharma and S. S. Chandel, "Performance and degradation analysis for long term reliability of solar photovoltaic systems: A review," *Renew. Sustain. Energy Rev.*, vol. 27, pp. 753–767, 2013.

[25] B. V Chikate and Y. . Sadawarte, "The Factors Affecting the Performance of Solar Cell," in *International Journal of Computer Applications (0975 – 8887)*, 2015, pp. 1–5.

[26] M. Z. Jacobson and V. Jadhav, "World estimates of PV optimal tilt angles and ratios of sunlight incident upon tilted and tracked PV panels relative to horizontal panels," *Sol. Energy*, vol. 169, no. April, pp. 55–66, 2018.

[27] S. S. Mohammed-, "Modeling and Simulation of Photovoltaic module using Matlab / Simulink," *Int. J. Chem. Environ. Eng. Model.*, vol. 2, no. 5, 2011.

[28] C. Sirisamphanwong and N. Ketjoy, "Impact of spectral irradiance distribution on the outdoor performance of photovoltaic system under Thai climatic conditions," *Renew. Energy*, vol. 38, no. 1, pp. 69–74, 2012.

[29] A. Dominguez, J. Kleissl, and J. C. Luvall, "Effects of solar photovoltaic panels on roof heat transfer," *Sol. Energy*, vol. 85, no. 9, pp. 2244–2255, 2011.

[30] H. Tsai, C. Tu, and Y. Su, "Development of Generalized Photovoltaic Model Using Matlab / Simulink," *Proc. World Congr. Eng. Comput. Sci. 2008 WCECS 2008, Oct. 22 - 24, 2008, San Fr. USA*, p. 6, 2008.

[31] H. Bellia, R. Youcef, and M. Fatima, "A detailed modeling of photovoltaic module using Matlab," *NRIAG J. Astron. Geophys.*, vol. 3, no. 1, pp. 53–61, 2014.

[32] L. Fara and D. Craciunescu, "Output Analysis of Stand-Alone PV Systems : Modeling , Simulation and Control," *Energy Procedia*, vol. 112, no. October 2016, pp. 595–605, 2017.

[33] J. C. Pradhan Arjyadhara, Ali S.M, "Analysis of Solar PV cell Performance with Changing Irradiance and Temperature," *Int. J. Eng. Comput. Sci.*, vol. 2, no. 1, pp. 214–220, 2013.

[34] C. Schwingshackl, M. Petitta, J. E. Wagner, G.

Belluardo, and D. Moser, “Wind effect on PV module temperature : Analysis of different techniques for an accurate estimation,” *Energy Procedia*, vol. 40, pp. 77–86, 2013.

[35] E. Skoplaki and J. A. Palyvos, “On the temperature dependence of photovoltaic module electrical performance : A review of efficiency / power correlations,” *Sol. Energy*, vol. 83, no. 5, pp. 614–624, 2009.

[36] K. Ishaque, Z. Salam, and H. Teheri, “Accurate MtLab Simulink PV System Simulator Based on a Two-Diode model,” *J. Power Electron.*, vol. 11, no. 2, 2011.